(4) J. E. Carless and A. A. Foster, *J. Pharm. Pharmacol.*, **18**, 697(1966).
(5) J. Glasby and K. Ridgway, *ibid.*, **20**, 94S(1968).
(6) H. Nogami and T. Nagai, *Yakkyoku*, **9**, 29(1958).
(7) J. Hasegawa and T. Nagai, *Chem. Pharm. Bull. (Tokyo)*, **6**, 129(1958).
(8) D. C. Grove and G. L. Keenan, *J. Amer. Chem. Soc.*, **63**, 97(1941).
(9) J. A. Biles, *J. Pharm. Sci.*, **50**, 464(1961).
(10) D. J. Allen, G. Milosovich, and A. M. Mattocks, *ibid.*, **54**, 383(1965).

ACKNOWLEDGMENTS AND ADDRESSES

Received June 4, 1969, from the *College of Pharmacy, University of Michigan, Ann Arbor, MI 48104*

Accepted for publication November 20, 1969.

Presented in part to the Basic Pharmaceutics Section, APhA Academy of Pharmaceutical Sciences, Dallas meeting, April 1966.

* Present address: Smith Kline & French Laboratories, Philadelphia, Pa.

Theoretical Model Studies of Drug Absorption and Transport in the Gastrointestinal Tract I

AKIRA SUZUKI, W. I. HIGUCHI, and N. F. H. HO

Abstract □ The simultaneous chemical equilibria and mass transfer of basic and acidic drugs through a two-phase compartment model were theoretically investigated. The model consisted of a well-stirred bulk aqueous phase, an aqueous diffusion layer, and a lipid barrier for perfect and imperfect sink cases. The nonsteady and quasi-steady-state changes in the concentration–distance distributions in the lipid phase were studied. The rate of change of the total drug concentration in the bulk aqueous phase was described in the general form of a first-order equation useful for the evaluation of experiments. A limiting steady-state relationship involving the transport rate with the partition coefficient, pH at the aqueous–lipid interface, dissociation constant of the drug, aqueous and lipid diffusion coefficients, and thickness of the diffusion layer was derived. Increasing the agitation rate in the aqueous phase markedly affects the pH profiles for the rate of transport. The pH-partition theory is shown to be a limiting case of the more general approach presented.

Keyphrases □ Drug absorption, transport—theoretical model □ Model, two-phase compartment—theoretical investigation □ Chemical equilibria, mass transfer—two-phase compartment model □ Agitation rate effect—rate transport pH profiles

The increasing interest in the mechanistic understanding rather than in only a mathematical representation of drug transport and absorption phenomena should dictate systematic physical model analyses of various *in vitro* situations. Thus, detailed theoretical considerations of diffusion and equilibria involving multibarrier systems and the carrying out of appropriate model experiments are necessary for the isolation of the important *in vivo* factors.

Recent investigations (1–4) in these laboratories have been devoted to the physical model approach to a number of situations in this regard. The present paper is concerned with the problem of treating the time dependency and the pH-buffer dependency for the transport of basic and acidic solutes into and across lipoidal barriers. It is, to some extent, an extension of the works of Howard *et al.* (3) and Stehle (4) and should be useful in the understanding of gastrointestinal and buccal absorption problems. In the accompanying paper (5), the techniques developed here are applied to some of the data on *in situ* drug absorption published by Koizumi *et al.* (6, 7).

THEORY

General Description of the Model—The simultaneous mass transfer and chemical equilibrium reactions in a system consisting of two homogeneous phases will follow the one-dimensional model in Fig. 1. The bulk aqueous phase is well stirred and consists of a basic drug and buffer. At $x \leq -h$,

$$(TR)_{-h} = (R)_{-h} + (RH^+)_{-h} \quad \text{(Eq. 1)}$$

$$(TB)_{-h} = (B^-)_{-h} + (HB)_{-h} \quad \text{(Eq. 2)}$$

where (TR) is the total drug concentration of R and RH^+ species and (TB) is the total buffer concentration of B^- and HB species. It is assumed that electrical neutrality holds everywhere in the aqueous phase. Consequently, at $x \leq 0$,

$$(H^+) + (RH^+) + (Na^+) - (OH^-) - (B^-) = 0 \quad \text{(Eq. 3)}$$

where (Na^+) is the cation concentration derived from the buffer. It is further assumed that the following equilibrium reactions are instantaneous,

$$\frac{(R)(H^+)}{(RH^+)} = K_{a,R} \quad \text{(Eq. 4a)}$$

$$\frac{(B^-)(H^+)}{(HB)} = K_{a,HB} \quad \text{(Eq. 4b)}$$

$$(H^+)(OH^-) = K_w \quad \text{(Eq. 4c)}$$

where $K_{a,R}$, $K_{a,HB}$, and K_w are the dissociation constants of drug, buffer, and water, respectively.

Under the assumption of quasi-steady-state conditions existing within the aqueous diffusion layer, the total flux of the drug to the water–lipid interface is expressed by the equation

$$G = -D_{RH}\frac{d(RH^+)}{dx} - D_R\frac{d(R)}{dx} \quad \text{(Eq. 5)}$$

$$(-h \leq x \leq -0)$$

where G is the total flux of the drug and D_{RH} and D_R are the diffusion coefficients; upon integration, the solution is

$$Gh = D_{RH}(RH^+)_{-h} + D_R(R)_{-h} - D_{RH}(RH^+)_{-0} - D_R(R)_{-0} \quad \text{(Eq. 6)}$$

In an analogous procedure for the buffer species,

$$D_{HB}(HB)_{-h} + D_B(B^-)_{-h} - D_{HB}(HB)_{-0} - D_B(B^-)_{-0} = 0 \quad \text{(Eq. 7)}$$

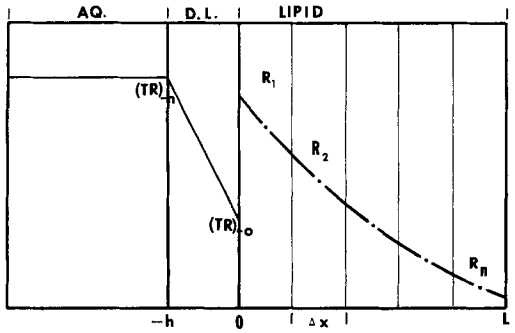

Figure 1—*Two-phase diffusion model consisting of a bulk aqueous phase, aqueous diffusion layer, and a lipid phase. Concentration distribution of total drug species is governed by steady-state rate into the diffusion layer, and concentration of the diffusing nonionized drug in the lipid phase is governed by nonsteady-state rate determined by numerical finite-difference methods.*

in which case the total flux of the buffer is zero.

If only the nonprotonated drug molecule is capable of diffusing into the lipid phase, the equilibrium assumed to be established instantaneously at the aqueous–lipid interface is expressed by the partition coefficient,

$$P = (R)_{+0}/(R)_{-0} \quad (x = 0) \qquad \text{(Eq. 8)}$$

where P is the partition coefficient; (R) is the concentration of the nonionized drug; and the subscripts, -0 and $+0$, refer to the aqueous and lipid side of the interface, respectively. The continuity of flow through the interface is given by

$$G = -D_{R,oil}\left(\frac{\partial(R)}{\partial x}\right)_{x=0} \qquad \text{(Eq. 9)}$$

where $D_{R,oil}$ is the diffusion coefficient of R in lipid. In this model the flux of the total drug species in the aqueous diffusion layer is taken to be the same as the flux of the nonionized drug from the interface to the lipid phase. Within the lipid, Fick's second law applies:

$$\frac{\partial(R)}{\partial t} = D_{R,oil}\frac{\partial^2(R)}{\partial x^2} \quad (x > 0) \qquad \text{(Eq. 10)}$$

and at $x = L$ two extreme boundary conditions can exist, that is, (*a*) for the impermeable boundary,

$$\left(\frac{\partial(R)}{\partial x}\right)_{x=L} = 0 \qquad \text{(Eq. 11}a\text{)}$$

(*b*) for the perfect sink,

$$(R)_{x=L} = 0 \qquad \text{(Eq. 11}b\text{)}$$

Changes in the Concentration–Distance Distribution in the Aqueous and Lipid Phases with Time—The simultaneous time change of the total drug concentration–distance distribution in the aqueous phase in which steady-state conditions are assumed and that for the diffusing basic drug molecule in the lipid phase in which nonsteady-state conditions exist cannot be solved analytically. Numerical methods and the utilization of a high-speed computer are necessary.

In using the finite-difference method (8), the lipid compartment is divided into a number of cells of equal intervals as shown in Fig. 1. Accordingly, the concentration of drug in the bulk aqueous phase and each cell in the lipid phase and at the interface can be calculated by solving the following set of differential equations:

$$\frac{d(TR)_{-h}}{dt} = -\frac{A}{V}G \qquad \text{(Eq. 12)}$$

$$\frac{d(R_1)}{dt} = \frac{G}{\Delta x} - \frac{D_{R,oil}[(R_1) - (R_2)]}{(\Delta x)^2} \qquad \text{(Eq. 13)}$$

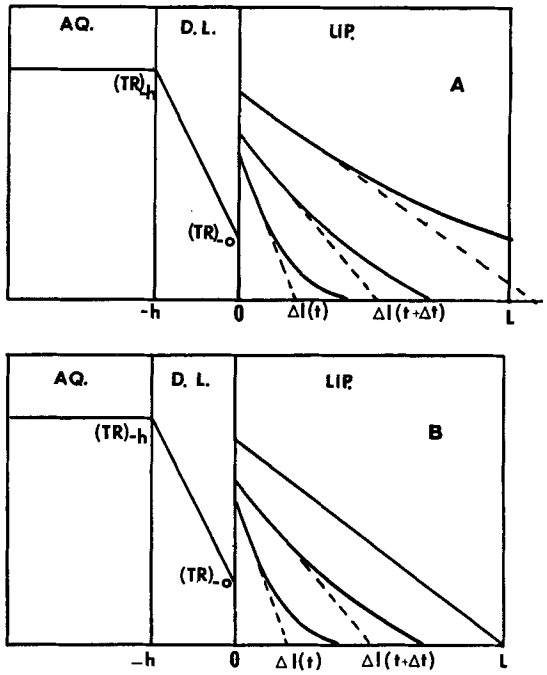

Figure 2—*Model used to estimate* F(t) *by linear approximation of the concentration–distance curves in the lipid phase. Key: A, impermeable boundary case; and B, perfect-sink case.*

$$\frac{d(R_i)}{dt} = \frac{D_{R,oil}}{(\Delta x)^2}[(R_{i-1}) - 2(R_i) + (R_{i+1})] \quad (i = 2, 3, 4 \ldots n-1) \qquad \text{(Eq. 14)}$$

and at $x = L$, for the impermeable boundary or no-sink case,

$$\frac{d(R_n)}{dt} = \frac{D_{R,oil}}{(\Delta x)^2}[(R_{n-1}) - (R_n)] \qquad \text{(Eq. 15}a\text{)}$$

and for the perfect-sink case,

$$\frac{d(R_n)}{dt} = \frac{D_{R,oil}}{(\Delta x)^2}[(R_{n-1}) - 3(R_n)] \qquad \text{(Eq. 15}b\text{)}$$

where A is the surface area, V is the volume of the bulk aqueous phase, (R_i) is the concentration of neutral drug in the ith cell, Δx is the length of each cell, n is the total number of cells, and the other terms are defined as before.

Since the concentration of drug species at the various aqueous boundaries is dependent upon pH, the hydrogen-ion concentration must be known. From Eqs. 1 through 4 the hydrogen-ion concentration in the bulk phase is given by

$$(H^+)^4_{-h} + \{K_{a,R} + K_{a,HB} + (TR)_{-h} + (Na^+)_{-h}\}(H^+)^3_{-h} + \{[(TR)_{-h} + K_{a,R} - (TB)_{-h}]K_{a,HB} - (K_{a,R} + K_{a,HB})(Na^+)_{-h}K_w\}(H^+)^2_{-h} - \{K_{a,HB}(TB)_{-h} + (K_{a,R} + K_{a,HB})K_w + K_{a,R}K_{a,HB}(Na^+)_{-h}\}(H^+)_{-h} - K_{a,R}K_{a,HB}K_w = 0 \qquad \text{(Eq. 16)}$$

Table I—Numerical Dimensions of Constants and Initial Drug and Buffer Concentrations Used for Computation

$V = 10$ cm.^{3}	$A = 10$ cm.^{2}	$h = 10^{-2}$ cm.
$K_{a,R} = 10^{-8}$	$D = 10^{-5}$ cm.^{2} sec.$^{-1}$ for all diffusion coefficients	
Initial concentrations: $(TB)_{-h} = 10^{-2}$ M		
$(TR)_{-h} = 10^{-4}$ M		

	No-Sink Case	Perfect-Sink Case
L	10^{-1} cm.	5×10^{-2} cm.
$(Na^+)_{-h}$	0	$^1/_2(TB)_{-h}$
P	1, 100	100
$pK_{a,HB}$	4, 6, 8, 10, 12	4, 6, 8, 10

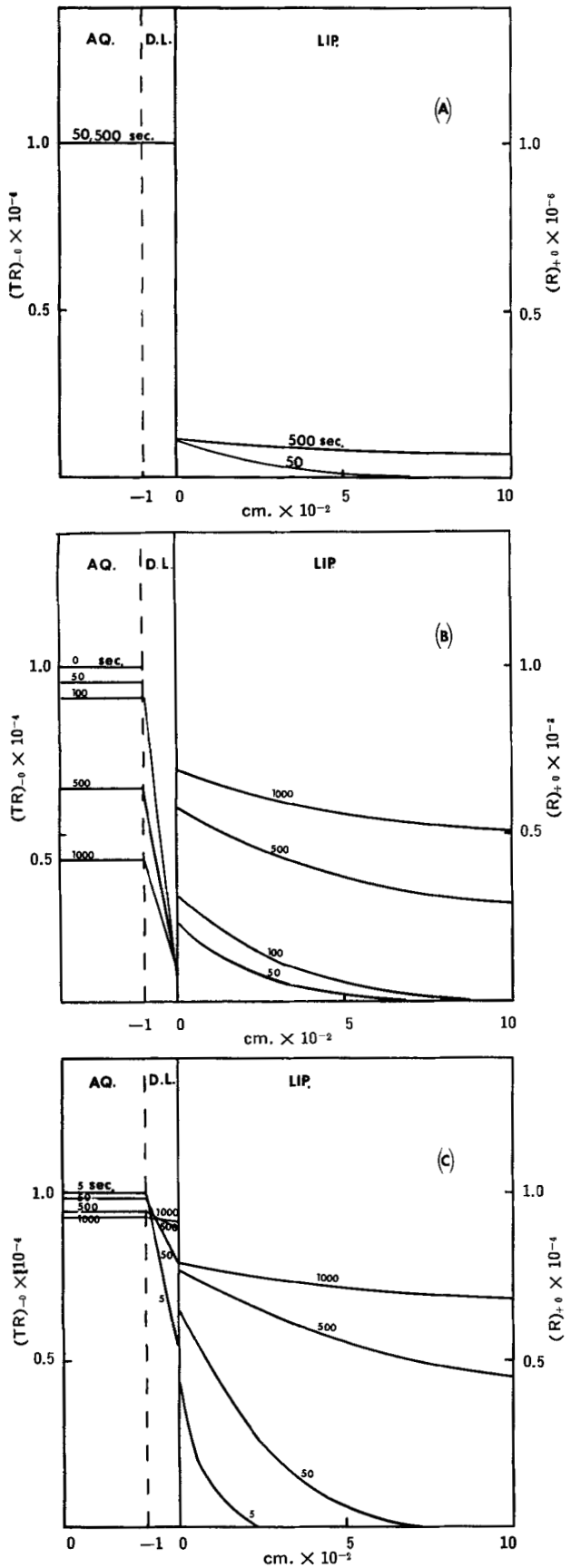

Figure 3—*Time-dependent concentration distribution curves of total drug species (TR) in the aqueous phase and the nonprotonated drug (R) in the oil phase for the no-sink case: (A) initial bulk aqueous pH = 3.05 and partition coefficient* P = *100; (B) pH = 8.82,* P = *100; (C) pH = 8.82,* P = *1.0.*

Table II—Change in the Bulk and Surface pH with Time for the No-Sink Case in a Low Buffer Capacity System with $P = 100$

$K_{a,HB}$	Initial pH$_{-h}$	Initial pH$_{-0}$	After 500 sec pH$_{-h}$	After 500 sec pH$_{-0}$
10^{-6}	3.05	3.05	3.05	3.05
10^{-8}	6.01	5.71	5.98	5.95
10^{-10}	7.79	6.84	7.67	7.33
10^{-12}	8.82	7.70	8.71	8.22

The equation for the hydrogen-ion concentration at the interface is derived from Eqs. 3, 4, and 6–9; thus,

$$(H^+)^4_{-0} + [\beta + \gamma\eta + \alpha + \gamma(Na^+)_{-0}](H^+)^3_{-0} + [(\alpha + \beta)\eta - \gamma K_w - \gamma\delta + (\gamma\eta + \beta)(Na^+)_{-0}](H^+)^2_{-0} - [(\beta + \gamma\eta)K_w - \beta\delta + \beta\eta(Na^+)_{-0}](H^+)_{-0} - \beta\eta K_w = 0 \quad \text{(Eq. 17)}$$

where

$$\alpha = \frac{1}{K_{a,R}}\left\{[D_R(R)_{-h} + D_{RH}(RH^+)_{-h}] + \frac{2hD_{R,oil}(R_I)}{\Delta x}\right\}$$

$$\beta = D_R + \frac{2hPD_{R,oil}}{\Delta x}$$

$$\gamma = D_{RH}/K_{a,R}$$

$$\delta = \frac{K_{a,HB}}{D_B}[D_B(B^-)_{-h} + D_{HB}(HB)_{-h}]$$

$$\eta = \frac{K_{a,HB}D_B}{D_{HB}}$$

Here, it is assumed that $(Na^+)_{-h} = (Na^+)_{-0}$. Finally, the concentration of the diffusing specie at the aqueous side of the interface, *i.e.* $(R)_{-0}$, is expressed by

$$(R)_{-0} = \frac{\alpha K_{a,R}}{\beta + \gamma(H^+)_{-0}} \quad \text{(Eq. 18)}$$

Rate of Change of the Total Concentration of Drug in the Bulk Aqueous Phase—To relate the theory of the diffusion model to the usual treatment of experimental data, *i.e.*, the rate of change of the total drug concentration in the bulk aqueous phase, it is useful to rewrite Eq. 12 in the following manner,

$$\frac{d(TR)_{-h}}{dt} = -\frac{AD_R}{Vh}F(t)(TR)_{-h} \quad \text{(Eq. 19)}$$

where $F(t)$ is defined as

$$F(t) = G/G_{max.} \quad \text{(Eq. 20)}$$

and

$$G_{max.} = \frac{D_R(TR)_{-h}}{h} \quad \text{(Eq. 21)}$$

Equation 20 is the ratio of the actual flux to the maximum flux which takes place when all of the drug species in the bulk aqueous phase is nonprotonated and the concentration of R at the interface is zero. By performing the integration, Eq. 19 becomes

$$\ln\frac{(TR)_{-h}}{(TR)_{-h,t=0}} = -\frac{AD_R}{Vh}\int_0^t F(t)dt \quad \text{(Eq. 22)}$$

$$(0 < F(t) \leq 1)$$

and by utilizing the mean-value theorem to evaluate the integral,

$$\ln\frac{(TR)_{-h}}{(TR)_{-h,t=0}} = -\frac{AD_R}{Vh}F(\Phi)t \quad \text{(Eq. 23)}$$

$$(0 \leq \Phi \leq t)$$

If $F(\Phi)$ is relatively invariant with Φ, an apparent first-order decrease in the drug concentration with time will be observed. In general, the slope of ln $(TR)_{-h}$ *versus t* plots is

$$K_u = -\frac{AD_R}{Vh}F(\Phi) \quad \text{(Eq. 24)}$$

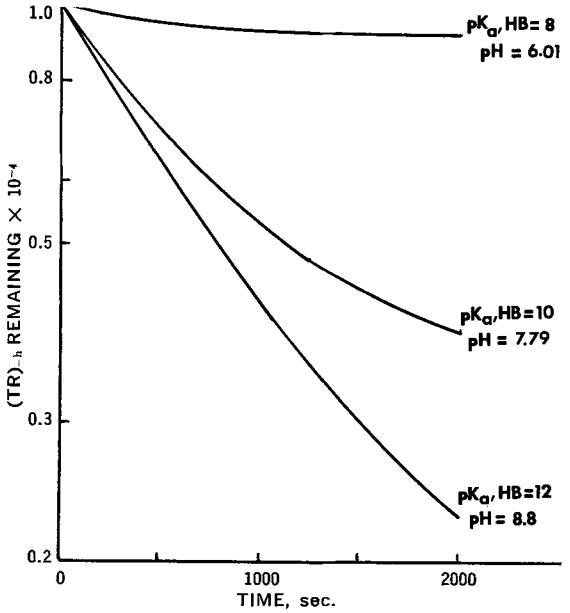

Figure 4—*First-order plot of the change in the total drug concentration in the bulk aqueous phase with time. No-sink case for different initial bulk aqueous pH.*

Approximation of the Function $F(t)$—Since the function $F(t)$ influences the apparent first-order rate constant, the elucidation of the nature of the function in terms of the partition coefficient, pH at the interface, diffusion coefficients, and thickness of the diffusion layer would lead to meaningful physical interpretation. For this purpose, an approximation of $F(t)$ is derived for two cases, perfect-sink and no-sink situations.

No-Sink Case—The analysis is based on the model for the concentration–distance distribution changes with time in Fig. 2A. It assumes a linear approximation of the nonsteady-state concentration profile of R at time t in the lipid phase. From Eqs. 8 and 9,

$$G = \frac{D_{R,oil}\, P(R)_{-0}}{\Delta 1} \qquad \text{(Eq. 25)}$$

where $\Delta 1$ is the distance from the interface to the point where $(R)_{+0}$ is zero and changes with time such that $0 < \Delta 1 > L$. Furthermore, assuming that the flux G has not changed appreciably during the period needed to build up the concentration distribution in the lipid phase, the total amount of drug transported through the interface is approximated by

$$\int_0^t G\, dt = \int_0^1 (R)_{oil}\, dx \qquad \text{(Eq. 26}a\text{)}$$

Thus,

$$Gt = \tfrac{1}{2}(R)_{-0} P \Delta 1 \qquad \text{(Eq. 26}b\text{)}$$

and it follows from Eqs. 25 and 26b that

$$\Delta 1 = (2D_{R,oil}t)^{1/2} \qquad \text{(Eq. 27)}$$

Solving for $(R)_{-0}$ with the aid of Eqs. 6 and 25 and $D_{RH} = D_R$,

$$(R)_{-0} = \frac{(TR)_{-h}}{1 + [(H^+)_{-0}]/(K_{a,R}) + (hD_{R,oil}P)/(\Delta 1\ D_R)} \qquad \text{(Eq. 28)}$$

and with Eq. 27,

$$(R)_{-0} = \frac{(TR)_{-h}}{1 + [(H^+)_{-0}]/(K_{a,R}) + (hD_{R,oil}P)/(D_R\sqrt{2D_{R,oil}t})} \qquad \text{(Eq. 29)}$$

It is convenient to define a new function $f(t)$ as the approximation of $F(t)$. By means of Eqs. 1, 4, 6, 20, and 21, the function can be simply expressed by

$$f(t) \sim F(t) = G/G_{max.} =$$

$$1 - \frac{\{1 + [(H^+)_{-0}]/(K_{a,R})\}(R)_{-0}}{(TR)_{-h}} \qquad \text{(Eq. 30)}$$

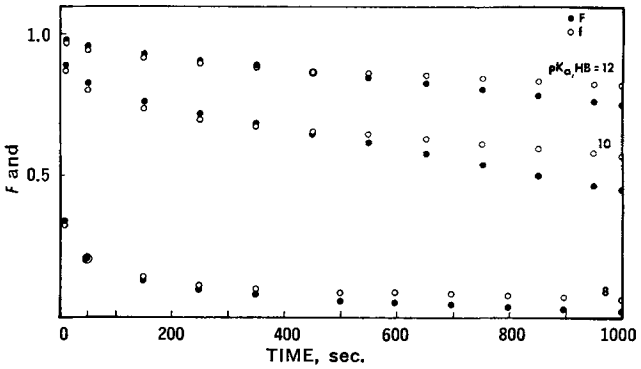

Figure 5—*Change in the diffusion efficiency coefficient with time for the no-sink case. The numerically calculated coefficient* F(t) *by Eq. 20 is compared with the approximation* f(t) *by Eq. 31.*

and the substitution of Eq. 29 leads to

$$f(t) = \frac{1}{\{1 + [(H^+)_{-0}]/(K_{a,R})\}\ T + 1} \qquad \text{(Eq. 31)}$$

where

$$T = \frac{D_R}{hP}\left(\frac{2t}{D_{R,oil}}\right)^{1/2} \qquad \text{(Eq. 32)}$$

Therefore, in this case of an impermeable boundary in the lipid phase, the time-dependent nature of the function $f(t)$ makes it evident that first-order diffusion kinetics are not applicable.

Perfect-Sink Case—In this situation the diffusion of the drug can be divided into two stages (Fig. 2B). The first stage is the period of nonsteady-state rate in the lipid phase leading to the second stage of quasi-steady-state conditions. In other words, $F(t)$ will eventually be constant (time independent) after an initial lag period.

In the nonsteady-state period the approximate function $f(t)$ given by Eqs. 31 and 32 can be applied. From Eq. 27, with $\Delta 1 = L$ always, the time lag is

$$\tau = \frac{L^2}{2D_{R,oil}} \qquad \text{(Eq. 33)}$$

where τ is the lag time, and L is the thickness of the lipid phase.

In the steady-state period, Eq. 25 can be rewritten as

$$G = \frac{D_{R,oil}P(R)_{-0}}{L} \qquad \text{(Eq. 34)}$$

After the substitution of Eqs. 21, 28, and 34 into 20, the function[1] $f(T)$ takes the same form as Eq. 31; that is,[2]

$$f(T) = \frac{1}{\{1 + [(H^+)_{-0}]/(K_{a,R})\}\ T + 1} \qquad \text{(Eq. 35)}$$

where, in this case,

$$T = \frac{D_R L}{PhD_{R,oil}} \qquad \text{(Eq. 36)}$$

Therefore, in the perfect-sink case, a log $(TR)_{-h}$ *versus* t plot should be linear after a lag period.

---

[1] Note that $f(t)$ is replaced by $f(T)$ since the function is time-independent in the steady-state period for the perfect-sink case.

[2] While this theoretical treatment is based on an amine drug, the following equation can also be derived in an analogous manner for an acidic drug, like a barbiturate,

$$f(t) = \frac{1}{\{1 + (K_{a,R})/[(H^+)_{-0}]\}\ T + 1} \qquad \text{(Eq. 35}a\text{)}$$

where $K_{a,R}$ is the dissociation constant of the acidic drug and T is either Eq. 32 or 36, depending upon the perfect- or no-sink case.

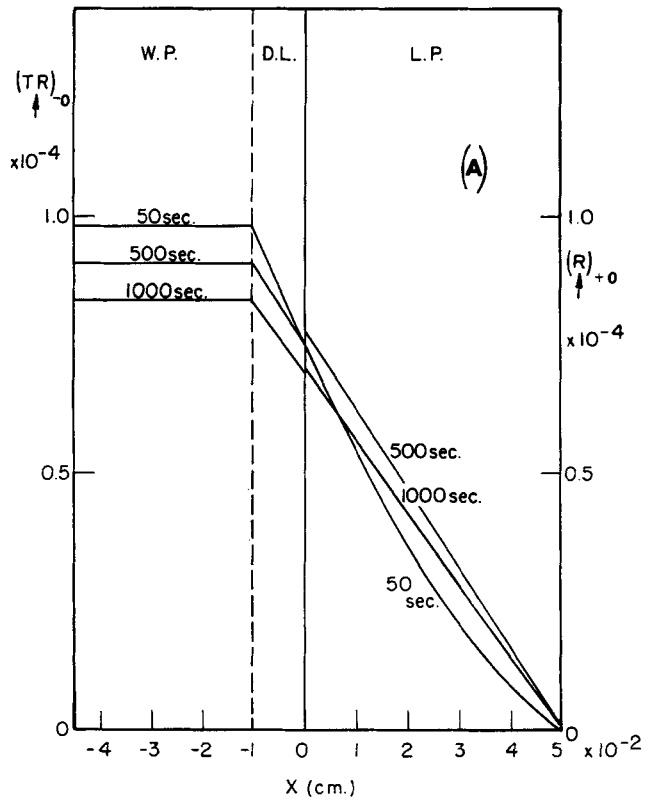

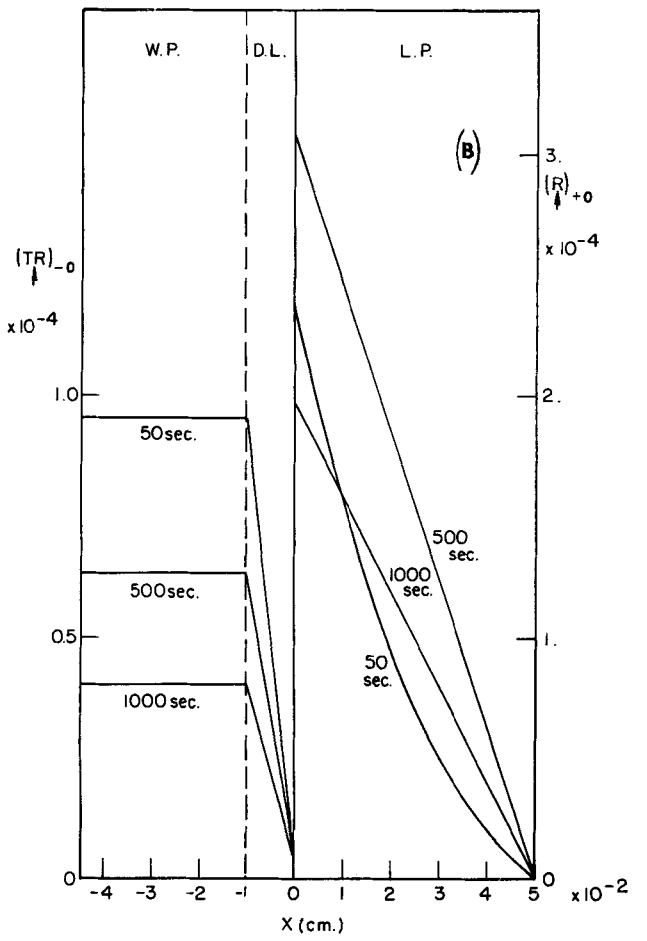

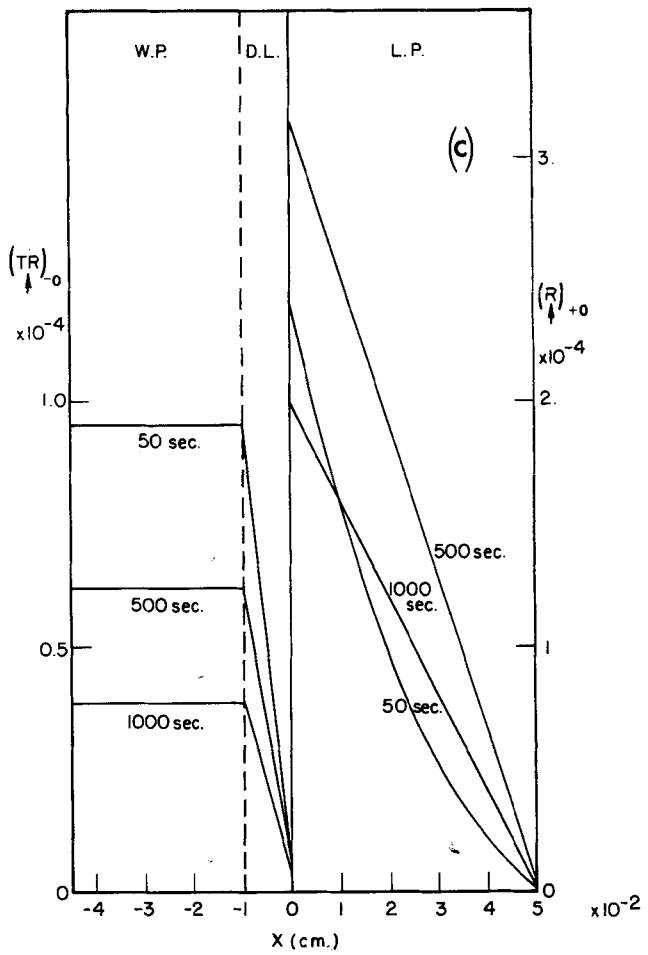

Figure 6—*Time-dependent concentration distribution profiles in aqueous and lipid phases for the perfect-sink case. Partition coefficient* P = *100. (A) Dissociation constant of buffer,* $K_{a,HB} = 10^{-6}$. *(B)* $K_{a,HB} = 10^{-8}$. *(C)* $K_{a,HB} = 10^{-10}$. *Sodium-ion concentration was one-half of the total buffer concentration always.*

CALCULATIONS

Computations were carried out for a range of parameters with the aid of the IBM 360/67 digital computer. Table I gives the dimensions of the constants and initial drug and buffer concentrations. The dissociation constant of the buffer and partition coefficient were varied. The detailed method of computation is given in the *Appendix*.

RESULTS AND DISCUSSION

In this section the interphase diffusional transport of an amine drug is analyzed for a wide range of pH and partition coefficients, other parameters being constant. It is discussed in relation to two extreme situations, the no-sink (impermeable lipid boundary at x = L) and the perfect-sink cases. In contrast to the later, the former case simulates the situation of retarded drug absorption in a simple way when the rate-determining step is due to one kind of interfacial barrier, like an impermeable membrane. There are also intermediate situations, *i.e.*,

$$\left(\frac{\partial(R)}{\partial x}\right)_{x=L} = C \qquad \text{(Eq. 37)}$$

where C is some nonzero value.

No-Sink Case—Typical changes of drug concentration–distance distribution curves in the aqueous and lipid phases with time are shown in Fig. 3. Steady-state and nonsteady-state conditions prevail

Table III—The Initial Slope K_u and $F(t)$ Values for the No-Sink Case with $P = 100$

$K_{a,HB}$	pH_{-h} at $t = 0$	K_u	$F(\Phi)$	$F(t)$	$f(t)$
10^{-4}	3.05	~0	~0	0.121×10^{-3}	0.157×10^{-3}
10^{-8}	6.01	0.123×10^{-3}	0.123	0.0973	0.1096
10^{-10}	7.79	0.736×10^{-3}	0.736	0.7163	0.6969
10^{-12}	8.82	0.915×10^{-3}	0.915	0.9053	0.8946

Table IV—Comparison of the Function $f(T)$ during the Steady-State Period and the Lag Time τ[a] with Theory for the Perfect-Sink Case in a Strong Buffer System

Initial			Steady-State		Lag Time, sec.	
$K_{a,HB}$	pH_{-h}	pH_{-0}	$F(T)$	$f(T)$	τ	$\tau_{obs.}$[b]
10^{-4}	4.03	4.03	2.16×10^{-3}	2.2×10^{-3}	125	100
10^{-6}	6.02	6.01	0.167	0.17	125	100
10^{-8}	8.01	8.00	0.902	0.91	125	100–200
10^{-10}	9.98	9.98	0.948	0.95	125	100–200

[a] τ calculated by Eq. 33. [b] $\tau_{obs.}$ estimated from Fig. 9.

in the respective diffusion layer and lipid phase. Because of the impermeable barrier, at sufficiently long times there will be a concentration buildup in the lipid that approaches some equilibrium concentration as determined by the partition coefficient.

Upon comparing Figs. 3A and B, the pH effect on the distribution profiles is evident. When $pK_{a,HB} = 4$ [and the bulk pH ~ 3 with $(Na^+) = 0$], the ratio of the initial bulk aqueous concentration of nonprotonated drug to the total concentration is only 1.11×10^{-5}. This results in a relatively small concentration gradient in the diffusion layer and, consequently, in a small amount of nonprotonated drug being transported into the lipid phase, even though the partition coefficient is favorable. On the other hand, when $K_{a,HB} = 10^{-12}$ (and the bulk pH ~ 8.8), the initial $(R)_{-h}/(TR)_{-h}$ is 0.887. Here the flux in the diffusion layer and the amount transported into the lipid are large. In Figs. 3A and C the results indicate that the rate of diffusion is influenced more by the amount of the free amine drug available for transport at the interface rather than the partition coefficient. In this regard, the pH profile of the diffusion model should be considered. Based on Eqs. 16 and 17, Table II shows the pH of the bulk aqueous phase and the interface for various $K_{a,HB}$ values and at different times with $P = 100$. Since $(Na^+) = 0$, the buffer capacity is very low. It is found that $pH_{-0} < pH_{-h}$ initially and can be explained by the fact that RH^+ and R species, as well as buffer, have some flux according to the concentration gradient within the diffusion layer and some RH^+ arriving at the interface dissociates into H^+ and R. The pH_{-h} will decrease in time and eventually will be equal to pH_{-0} when the diffusion rate is zero.

The semilogarithmic plots of $(TR)_{-h}$ *versus* t (Fig. 4) do not show a true linear relationship, as expected from Eq. 22, since the slope K_u is time dependent. When pH_{-0} of the system is approximately equal to or greater than the pKa of the drug, the initial rate is very rapid; however, due to the backup drug concentration in the lipid later on, the rate approaches zero. In Table III the initial apparent first-order rate constant is given and the function F, determined in various ways for the first 250-sec. period, shows good agreement. $F(\Phi)$ was calculated by using Eq. 23 and the initial slope from Fig. 4, $F(t)$ by the computer-simulated transport program from the general Eqs. 20 and 21, and $f(t)$ by Eqs. 31 and 32. However, in Fig. 5 the functions F and, therefore, the rate constants are always changing with time. That the rate constant in early period (~ 500 sec.) from the log $(TR)_{-h}$ *versus* t plot is apparently constant with time can be explained by the fact that it is less sensitive to time than the differentially calculated K_u. Also, after 500 sec., the $F(t)$ and $f(t)$ tend to diverge. Since the derivation of $f(t)$ is based on a linear approximation of the flux in the lipid (see Fig. 2A), the function $f(t)$ becomes a poorer approximation of $F(t)$ when backup occurs in the lipid compartment at the impermeable boundary.

Perfect-Sink Case—In Fig. 6 the concentration distribution curves are shown for various values of $K_{a,HB}$ with P = 100. Nonsteady-state diffusion in the lipid occurs in the initial period. Later, when the concentration–distance profile is linear, the system is at steady state and the diffusional rate is first order with respect to the total drug concentration in the bulk aqueous phase (Fig. 7). From Fig. 8, which shows the time change in $(TR)_{-h}$ and Q, the amount of nonprotonated drug in the sink, the lag time can be obtained by extrapolation and also predicted by Eq. 33. The results of this perfect-sink case are summarized in Table IV. Because of the strong buffer capacity, $(Na^+)_{-h} = (Na^+)_{-0} = 1/2(TB)$, the pH of the bulk aqueous phase and at the interface is nearly the same. There is good agreement between the lag time values obtained from the theory and the computer-simulated experiments and between the steady-state rate constants obtained in part from rigorous calculation by Eq. 19 and the approximation by Eqs. 35 and 36. Referring to Fig. 9, one can readily follow the course of the interphase transport by an analysis of $f(T)$. The curve is characterized by a rapid change with time, followed by an asymptotic relationship during the steady-state period. As the pH is more alkaline, the function $f(T)$ approaches 1 and the apparent first-order rate constant increases in magnitude.

Significance of the Function $f(T)$ for the Perfect-Sink Case—Thus far, the rate-determining factors have been discussed from the general viewpoint of the partition coefficient and the pH at the interface influencing the amount of nonionized drug available

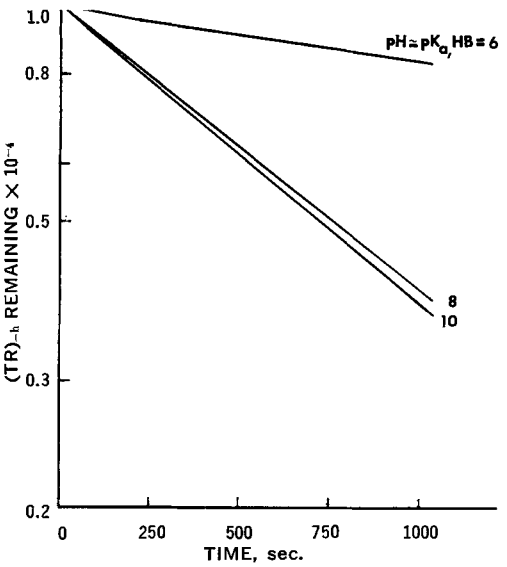

Figure 7—*First-order change in the total drug concentration in the bulk aqueous phase with time. Perfect-sink case for different initial bulk aqueous pH.*

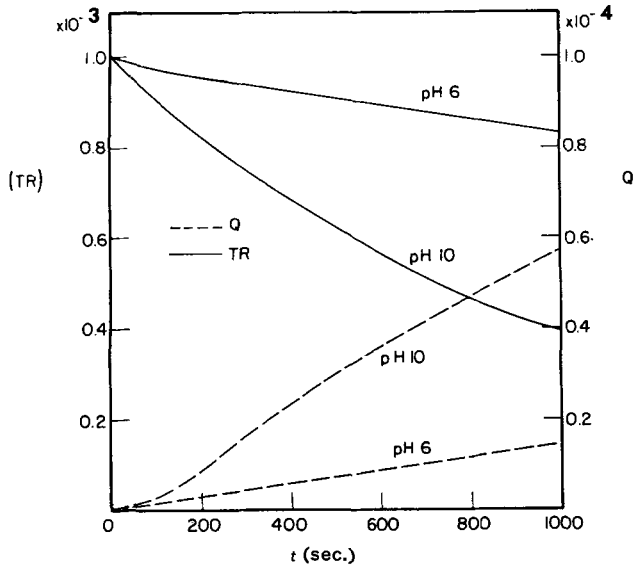

Figure 8—*Time change in the total amount of drug in the bulk aqueous phase and in the sink.*

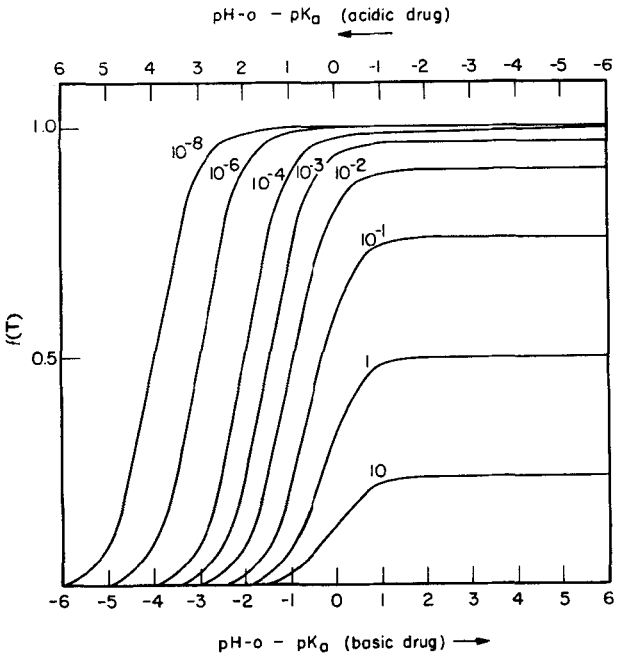

Figure 10—*Relationship of the pH at the aqueous–lipid interface and the pK of the drug with the diffusion efficiency coefficient for various T, which includes all transport parameters such as diffusion and partition coefficients, thickness of diffusion layer, and lipid phases.*

for diffusion across the lipid phase. It is useful to examine the nature of the time-independent function $f(T)$ by Eqs. 35 and 36 and the steady-state rate constant K_u (Eq. 24) relative to pH_{-0}.

As shown in Fig. 10, when the (pH_{-0} − pK_a) for a basic drug becomes increasingly positive and T is sufficiently small, say 10^{-6} to 10^{-8}, $f(T)$ is unity in the limit. Consequently, a few selected and interesting cases can be pointed out. If

$$\lim f(T) = 1, \quad \text{then } K_u = -\frac{AD_R}{Vh}$$

$$P \to \infty$$

$$(H^+)_{-0} \lesssim K_a$$

h = constant

On the other hand, if

$$\lim f(T) = 1, \quad \text{then } K_u \sim 0$$

$$h \to \infty$$

$$P \to \infty$$

$$(H^+)_{-0} \lesssim K_a$$

In both of these cases the rate-determining factor is the flux across the aqueous diffusion layer. These examples emphasize the importance of the aqueous diffusion layer, which is affected by the degree of stirring or agitation. More significantly, it shows that the pH-partition theory (9) is only a special case of the theory presented here. A very small value of $D_{R,oil}$ can also slow down the rate. In accordance with the pH-partition theory, the $f(T)$ and, consequently, $K_u \sim 0$ when the (pH_{-0} − pKa) becomes more negative.

Another interesting point in Fig. 10 is the shifting of the $f(T)$ *versus* (pH_{-0} − pKa) profiles with various T values. For T = 10, the profile approaches the dissociation curve characteristic of the basic drug; for other T values the profile deviates to the left of the dissociation curve.

From Eq. 36 it can be seen that increasing the partition coefficient, increasing h, increasing $D_{R,oil}$, decreasing D_R, or decreasing L, all have the effect of shifting the profile leftward away from the dissociation curve. The effect of agitation mentioned previously is particularly noteworthy in this regard. Thus it is important for investigators to recognize that the degree of agitation may not only influence the drug-absorption rate but that it can significantly influence the rate *versus* pH profiles. Another interpretation of the curves in Fig. 10 can be given; that is, at a constant diffusion layer thickness and a given rate of diffusion, the effect of a low concentration of non-

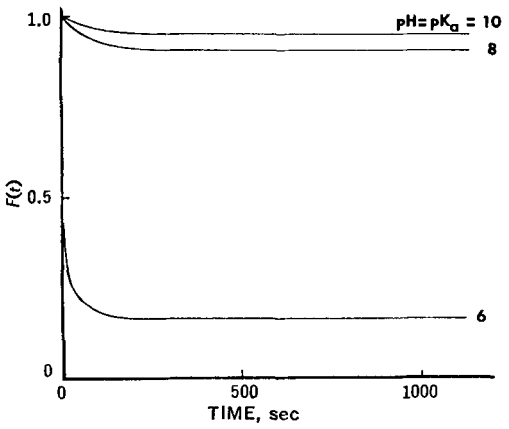

Figure 9—*Change in the diffusion efficiency coefficient with time for the perfect-sink case. After lag time,* F(t) *calculated is the same as the approximation* f(t).

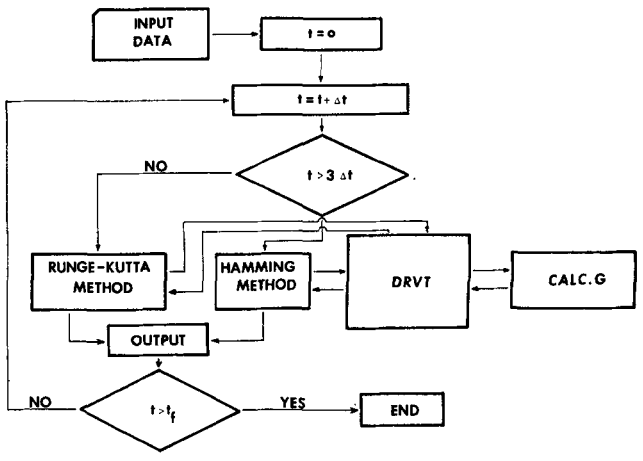

Scheme I—Flow diagram for the computation of concentration distributions

ionized species at the interface is balanced by a high partition coefficient and vice versa. All of these conclusions also apply to the case of acidic drugs in an analogous way.

In the study of rat intestinal and gastric absorption of sulfonamides, Koizumi *et al.* (6, 7) derived a first-order rate constant,

$$K_u \sqrt{M} = \frac{abP}{1 + aP} \qquad \text{(Eq. 38)}$$

where M is the molecular weight of the sulfonamide, K_u is the absorption rate of the nonionized moiety, a and b are constants, and P is the partition coefficient.

Equation 38 was found to be in good agreement with a large number of *in situ* experiments. It is noteworthy that the substitution of Eq. 35 or 35*a* into 24 gives

$$K_u = -\frac{AD_R}{Vh} \cdot \frac{BP}{1 + BP} \qquad \text{(Eq. 39)}$$

Both equations have the same form, although the methods of derivation are different. In the next paper, the results of Koizumi *et al.* and others will be discussed and compared with a similar model as presented in this study but modified to simulate the gastric and intestinal membrane.

APPENDIX

Numerical Calculating Procedure—To calculate the change of $(TR)_{-h}$, the concentration profile of R in the lipid phase with time and other parameters, the procedure shown in Scheme I is used. The input data are given in Table I. After $t = 0$, a series of calculation procedures undergo integration for each time increment, $t + \Delta t$. The $(TR)_{-h}$ and (R_i) at time t are determined by the stepwise integration of Eqs. 12–15*a* or 15*b*, depending upon the choice of the perfect-sink or no-sink case, by the Runge-Kutta technique for the initial period, $t \leq 3\Delta t$, and thereafter by the predictor-corrector method of Hamming (10). The calculation of the derivatives in Eqs. 12–15 is performed in the subroutine DRVT after evaluating G in the subroutine CALCG.

The procedure of subroutine CALCG is as follows. The first step involves the calculation of $(H^+)_{-h}$ from the fourth-power polynominal Eq. 16 by the Newton-Raphson method. Then $(R)_{-h}$, $(RH^+)_{-h}$, $(B^-)_{-h}$, and $(HB)_{-h}$ are obtained from Eqs. 1, 2, and 4, respectively. The next step is the evaluation of $(H^+)_{-0}$ from Eq. 17. In turn, $(B^-)_{-0}$, $(HB)_{-0}$, $(RH^+)_{-0}$ and $(R)_{-0}$ are found, using Eqs. 4, 7, and 18 and finally G by Eq. 6.

REFERENCES

(1) A. H. Goldberg, W. I. Higuchi, N. F. H. Ho, and G. Zografi, *J. Pharm. Sci.*, **56,** 1432(1967).

(2) A. Ghanem, W. I. Higuchi, and A. P. Simonelli, *ibid.*, **58,** 165(1969).

(3) S. A. Howard, A. Suzuki, M. A. Farvar, and W. I. Higuchi, to be published.

(4) R. G. Stehle and W. I. Higuchi, *J. Pharm. Sci.*, **56,** 1367(1967).

(5) A. Suzuki, W. I. Higuchi, and N. F. H. Ho, *ibid.*, **59,** 651(1970).

(6) T. Koizumi, T. Arita, and K. Kakemi, *Chem. Pharm. Bull.*, **12,** 413(1964).

(7) *Ibid.*, **12,** 421(1964).

(8) J. Crank, "Mathematics of Diffusion," Oxford, New York, N. Y., 1956.

(9) P. Shore, B. Brodie, and C. Hogben, *J. Pharmacol. Exp. Ther.*, **119,** 361(1957).

(10) A. Ralston and H. Wilf, "Mathematical Methods for Digital Computers," Wiley, New York, N. Y., 1960.

ACKNOWLEDGMENTS AND ADDRESSES

Received July 22, 1969, from the *College of Pharmacy, University of Michigan, Ann Arbor, MI 48104*

Accepted for publication December 16, 1969.

Presented to the Basic Pharmaceutics Section, APhA Academy of Pharmaceutical Sciences, Montreal meeting, May 1969.

Theoretical Model Studies of Drug Absorption and Transport in the Gastrointestinal Tract II

AKIRA SUZUKI*, W. I. HIGUCHI, and N. F. H. HO

Abstract □ Multicompartment diffusional models for the absorption of neutral, acidic, basic, and amphoteric drugs were investigated. The general model consisted of a bulk aqueous phase, an aqueous diffusion layer, n-compartments of homogeneous and heterogeneous phases, and a perfect sink. With the mathematical techniques reported previously, equations were derived in general terms for the nonsteady- and steady-state periods. Utilizing the steady-state diffusion efficiency function of the barrier systems, the first-order rate constants for various examples of two- and three-compartment models were obtained from the general model and some computations were given. Various sets of *in situ* experimental rat data have been analyzed by means of the different models. These include the intestinal, gastric, and rectal absorption of sulfonamides and barbituric acid derivatives. Self-consistent dimensional constants and diffusion coefficients were arrived at and the correlations obtained with the models have been found to be generally satisfactory.

Keyphrases □ Theoretical models—drug absorption, transport, gastrointestinal tract □ Drug absorption, transport, gastrointestinal tract—theoretical models, equations derived □ Kinetics—drug absorption, transport □ Sulfonamides—absorption, diffusion data, rats □ Barbituric acid derivatives—absorption, diffusion data, rats

In a previous paper the diffusion of basic and acidic drugs across an aqueous diffusion layer and a lipid compartment in a homogeneous two-phase model was presented (1). It provided a mathematical technique whereby more complicated models can be handled. A function was also derived which was found useful in analyzing the diffusion rate with respect to the partition coefficient, surface and bulk pH, dissociation constant, diffusion coefficients, and diffusion layer thickness.